Tellus (2003), 55A, 232–246

TELLUS
ISSN 0280–6495

Relevance of sub-grid-scale land-use effects for mesoscale models

By K. HEINKE SCHLÜNZEN[1]* and JACK J. KATZFEY[2], [1]*Meteorological Institute, University of Hamburg, Bundesstrasse 55, 20146 Hamburg, Germany;* [2]*CSIRO Atmospheric Research, PMB1, Aspendale, VIC 3195, Australia*

(Manuscript received 6 March 2002; in final form 3 December 2002)

ABSTRACT

The dependence of the performance of mesoscale-α and mesoscale-β models on model resolution and parameterisation of sub-grid-scale land-use effects is investigated for a meteorological situation that is strongly influenced by local effects. Two mesoscale models of different horizontal resolution and model physics are applied to the same meteorological situation, and the results are compared with observations. Sensitivity studies are performed to estimate the effect of resolution (4 km or 5 km versus 18 km), parameterisation of sub-grid-scale land-use effects and initial state on the results of both models. Results show that the accuracy improves with resolution when simple parameterisations of sub-grid-scale land-use effects are applied. The inclusion of sub-grid-scale land-use effects with application of a flux aggregation method provides the best solution, which is nearly independent of the resolutions used. The use of parameter averaging to account for sub-grid-scale land-use effects was worse than just using one (main) land-use per grid cell. Initial conditions were also found to have a significant impact on the results.

1. Introduction

Many global and regional climate models do not include parameterisations for multiple sub-grid-scale land-use effects. In contrast, some high resolving mesoscale-β models that have a horizontal resolution of kilometres include parameterisations for sub-grid-scale land-use effects (i.e. Klink, 1995; Mölders et al., 1996; von Salzen et al., 1996). This is at first surprising, since it might be expected that models of a higher resolution need less sophisticated parameterisations of sub-grid-scale effects, because these are partly resolved in the higher resolving models. However, model studies have shown that an increased resolution does not necessarily improve the model results (i.e. Bélair et al., 1998). Reasons for this are not fully clear, but shortcomings in the parameterisations applied are a very probable one reason. Support for this thesis can also be derived from results of mesoscale-β model studies. These have shown that the horizontal scale of sub-grid-scale land-use types needs to be considered in the parameterisations applied in mesoscale-β models (i.e. Arola, 1999; Lynn et al., 1995; Zeng and Pielke, 1995; Klink and Willmott, 1994). The dependence of land-use representation on horizontal resolution and model type has not been investigated extensively up to now.

The objective of this paper is to investigate the relevance of model resolution and sub-grid-scale land-use effects for the performance of mesoscale-α and mesoscale-β models. For this purpose sensitivity studies with respect to horizontal resolution and initial data have been performed with the Division of Atmospheric Research limited area model DARLAM (Section 3.1) and the mesoscale transport and stream model METRAS (Section 3.2). Results are compared with observations and with results of the sensitivity studies. Studies performed with METRAS test the impact of different parameterisations for including

*Corresponding author.
e-mail: schluenzen@dkrz.de

sub-grid-scale land-use effects on model performance. Both models are applied to the same meteorological situation. For the case study, a situation was selected that is dominated by local effects (see Section 2) to detect sub-grid-scale influences more clearly. The evaluation method is given in Section 4, and results are presented in Section 5.

2. Meteorological situation and comparison data

The simulations were performed for an evaluation area around Berlin, Germany (Fig. 1). The orography (USGS, 1996) is generally flat, ranging from 1 m above sea level at a minimum to a maximum of about 200 m. Therefore, the influence of the orography will be small. In particular, the shading effect by mountains will only be noticeable within about a kilometre of steeper terrain and close to sunrise and sunset.

The land-use data have been derived from an EU Coordination of Information on the Environment (CORINE) land-use data set for north-west Europe on a 30″ grid (Smiatek, 1998). Small-scale heterogeneous land-use dominates the evaluation area (53%; Fig. 2a), but coniferous forest is quite frequent too (22%). Meadows (7%), urban/sub-urban regions (6%) and mixed forest (6%) cover altogether 19% of the area. Less frequent land-use types are heath (2%), bushes (1%), lakes (2%) and non-vegetated areas of sand (1%). When focusing on the main land-use on a 4 km grid (Fig. 2b), the proportion of the heterogeneous mixed land-use increases to 65% and of coniferous forest to 24%. All other land-uses are less frequent: meadows, urban/sub-urban regions and mixed forest cover altogether about 9% and the remaining ones only 2% of the area.

22 July 1994 was selected for the evaluation, on which day a ridge was situated over the Baltic Sea with generally easterly flow over northern Germany (Fig. 3). Weak pressure gradients associated with the anticyclone caused light wind conditions (wind speeds were generally less than 3 m s^{-1}) and little cloudiness, resulting in maximum air temperatures of more than 30 °C in the investigation area. The influence of the anticyclone also resulted in a low surface humidity, with dew point temperatures of around 10 °C. This situation was quite steady for several days prior to the day chosen. The persistence of the situation can also be seen from Fig. 4, which shows the radiosoundings data taken at Lindenberg. Stratification, humidity and wind profiles remain very similar within the selected period.

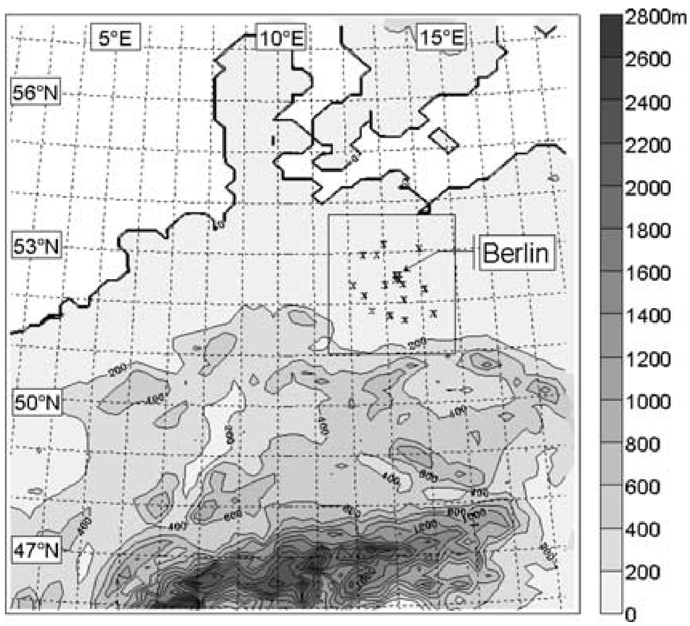

Fig. 1. DARLAM 18-km domain with orography (in m) shaded and the DARLAM 5-km domain noted by the box, which is also approximately the domain used for the METRAS model. Measurement sites are noted with '×'.

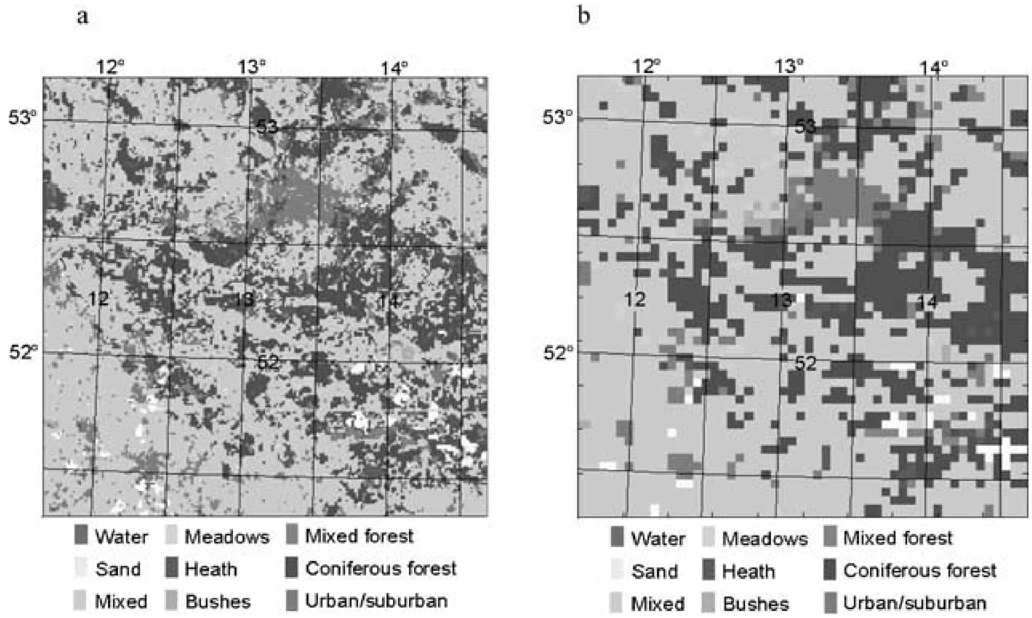

Fig. 2. (a) Land-use types within the evaluation area in a 1-km resolution based on the CORINE 30″ data set (Smiatek, 1996).(b) Main land-use type in the METRAS 4-km evaluation area.

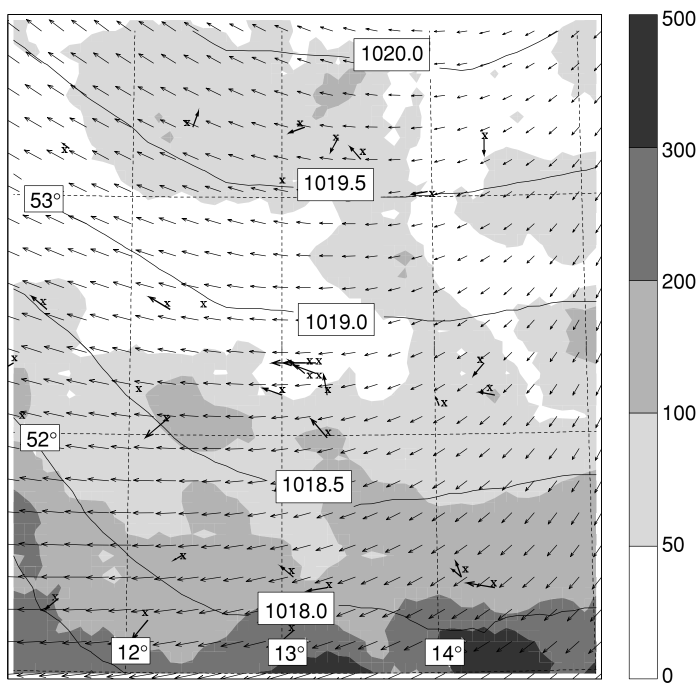

Fig. 3. ECMWF mean sea-level pressure (every 0.5 hPa) and 40-m wind vectors with observed wind vectors overlaid (dark) for 1200 UTC, 22 July 1994, for the evaluation area marked in Fig. 1. Analysis data interpolated to the 5-km DARLAM grid. Shading is orography in m.

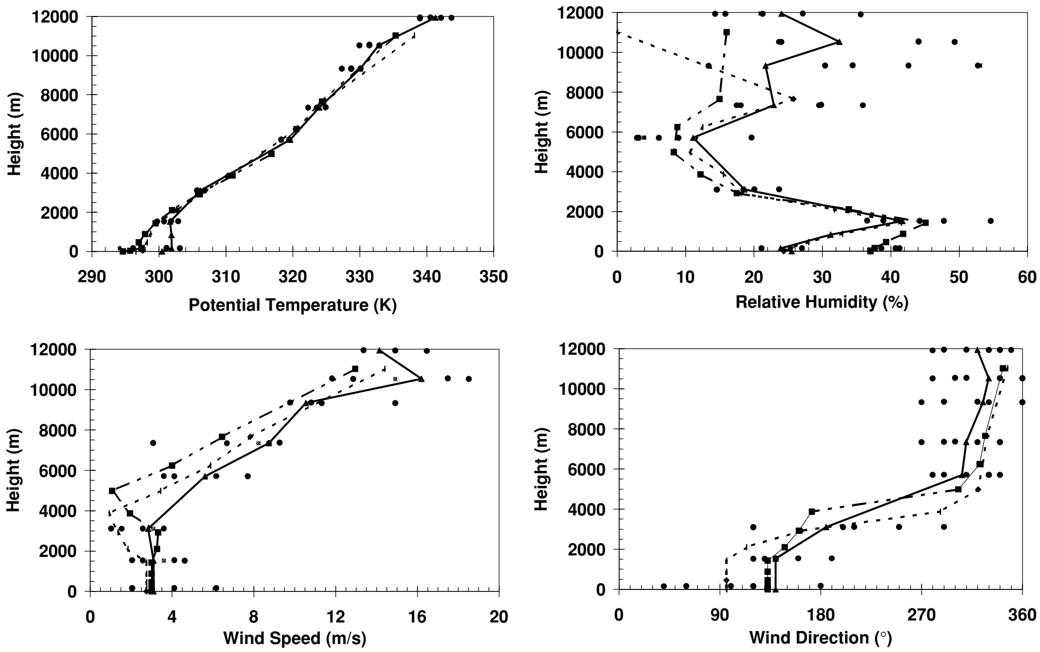

Fig. 4. Rawinsonde data (dots) from Lindenberg from 21 July 1994 (1800 UTC) to 23 July 1994 (0000 UTC), the average sounding (solid line) to initialise the METRAS 1-D model, and profiles derived from NCEP (dashed line) and ECMWF (dashed-dotted line) analysis data to initialise METRAS.

The selected day is characterised by a very dry, low-wind-speed and a steady large-scale situation. In these conditions the influence of land use on the boundary-layer development and on the diurnal cycle of temperature and humidity is at a maximum. This situation is therefore best suited to investigate the effect of sub-grid-scale land use on the meteorological parameters calculated at the surface.

For comparison routine surface measurements of temperatures and dew-point temperatures, wind (direction and speed) and pressure at 18 sites are used (see Fig. 1; routine data from "Deutscher Wetterdienst"). Most sites provide hourly data, though some only had data with a three-hourly interval. The approximate 380 measurements per parameter were carefully checked for plausibility (see Section 4).

3. Model description

The two models applied are based on the same equations, but differ in applied approximations, solution of the equations (numerical schemes, grid structure) and in the parameterisations used.

3.1. DARLAM

The Division of Atmospheric Research limited-area model (DARLAM) was designed for regional climate modelling studies (McGregor et al., 1993). It has also been applied to case studies of extreme orographic rainfall (Katzfey, 1995) and used in cloud system studies (Katzfey and Ryan, 1996; 2000) as well as for high-resolution modelling of pollution transport.

3.1.1. Equations and parameterisations of DARLAM. DARLAM is a two-time-level, semi-implicit, hydrostatic, sigma (pressure) coordinate, primitive equations model with semi-Lagrangian horizontal advection on an Arakawa C-grid (McGregor, 1987; 1993; McGregor et al., 1993). In these simulations, a three-layer soil model is used for temperature using the scheme of Kowalczyk et al. (1991), and moisture at two soil levels was predicted, using the force-restore method of Deardorff (1978). For computation of surface heat and moisture fluxes each grid box is assigned a fractional coverage of one main land-use type, with the rest of the grid box assumed to be bare soil. No explicit account is taken for understorey vegetation such as grass, although some land use types implicitly account for a grass understorey in the parameters specified for the land use. Hence, as is shown in Section 5.3, large soil moistures are required by the model to account for the transpiration of any understorey. The surface fluxes are calculated with a modified Louis (1979) parameterisation using a leaf area index weighted average of the vegetation and bare ground fluxes. Prior to model execution, the roughness length of the vegetation component over land was computed using an area weighted logarithmic average of the roughness lengths associated with the various vegetation types of the high-resolution input land-use dataset within each model grid cell:

$$z_0 = \exp\left(\sum \frac{(\text{area of land use}) \times \ln(z_{0,\text{ land use}})}{(\text{area of grid cell})}\right)$$

During model execution, the evaporation from the vegetated fraction of the grid cell was computed using only vegetation parameters from the primary land-use. Charnock (1955) is used to calculate roughness lengths over the ocean. Roughness lengths for momentum are 7.4 times that for heat

The numerical model uses the Geophysical Fluid Dynamics Laboratory's radiation package described in Schwarzkopf and Fels (1991) for longwave radiation and Lacis and Hansen (1974) for shortwave radiation with relative humidity-based diagnosed clouds. The outermost grid points are relaxed towards the analyses via the Davies (1976) type scheme, but modified so that the weights decrease exponentially inward from the lateral boundary. The simulations employ a mass-flux convection parameterisation, modified from the Arakawa (1972) scheme.

3.1.2. Description of the DARLAM model simulations. The data used as initial and boundary values were either the six-hourly NCEP re-analysis or the standard 12-hourly ECMWF analyses. Both analyses were first horizontally interpolated to the model grid using a bi-cubic interpolation. The surface pressure field was then computed using the pressure levels and geopotential heights to compute the surface pressure on the model orography. The data were then vertically interpolated to the 18 model sigma levels. The lateral boundary conditions were linearly interpolated in time from the available data (six-hourly from NCEP, 12-hourly from ECMWF). The 18-km simulations were nested within analyses, and the 5-km simulation then nested within the 18-km simulation. In the lowest 2000 m of the atmosphere, there are five layers at approximately 45, 220, 540, 1000 and 1570 m.

The initial soil temperatures and soil moistures were interpolated from the NCEP re-analysis data, since appropriate data were not available from the ECMWF analysis. In some simulations (see Table 1) the minimum soil moisture was set to about 90% of field capacity, as it was decided through the sensitivity studies presented in Section 5.3 that the NCEP soil moisture was too dry for the DARLAM simulations. The surface temperature was used from either the NCEP or ECMWF data sets.

Table 1. *Characteristics of the DARLAM (D1–D5) and METRAS (M1–M8) model simulations*

Case	Resolution (km)	Initialisation/boundary condition	Soil moisture initialisation	Sub-grid-scale land use	Sub-grid-scale fluxes
D1	18	ECMWF/ECMWF	NCEP, minimum soil moisture 90% of field capacity	One vegetation type and bare ground	Logarithmic average of z_0
D2	18	Same as D1	NCEP	Same as D1	Same as D1
D3	5	ECMWF/D1	Same as D1	Same as D1	Same as D1
D4	18	NCEP/NCEP	Same as D1	Same as D1	Same as D1
D5	18	NCEP/NCEP	NCEP	Same as D1	Same as D1
M1	4	Measured profile/lateral open	See Table 2	Yes	Flux aggregation
M2	18	Same as M1	See Table 2	Yes	Flux aggregation
M3	4	Same as M1	See Table 2	Yes	Parameter averaging
M4	18	Same as M1	See Table 2	Yes	Parameter averaging
M5	4	Same as M1	See Table 2	No	not relevant
M6	18	Same as M1	See Table 2	No	not relevant
M7	4	ECMWF profile/lateral open	See Table 2	Yes	Flux aggregation
M8	4	NCEP profile/lateral open	See Table 2	Yes	Flux aggregation

As will be shown, the initialisation of the soil moisture (and temperature) was critical for these short-term simulations. When DARLAM is used for in-house weather predictions, the soil moisture and temperatures are used from the previous forecast run in an attempt to initialise them with hopefully realistic values. Since these forecasts were not available for this time period, the NCEP re-analyses values were used. However, these values are highly dependent upon the soil scheme used in the re-analysis and are not based on observations. After evaluation of the simulations using these values, the regions of low soil moisture were increased to 90% of field capacity in order to have a better simulation of the dew-point temperature.

The surface albedo was set to 20% everywhere, since high-resolution observed data sets were not available. The soil was characterised as clay loam/silt loam everywhere. The main land-use type found was characterised as crops and trees, although other regions, in decreasing coverage, were classified as deciduous trees, small trees with ground cover, mixed trees and finally only ground cover. The surface roughness length for momentum varied in the verification area from 0.05 to 0.34 m. The stomatal resistance was set to values appropriate for the land use applied. All simulations were performed with each grid cell having one primary land-use type and bare ground. The fluxes are area weighted by the vegetation fraction. Multiple sub-grid-scale land-use types were not considered.

The DARLAM model results corresponding to the measurement sites were from the nearest model grid-point value. In the vertical, atmospheric values (2 m temperature and moisture values and 10 m wind values) were computed using the vertical profile as computed by the models' boundary layer scheme. Surface pressure was reduced to sea level using the standard lapse rate.

3.2. METRAS

The mesoscale transport and fluid model METRAS can be used for simulation areas between $10 \times 10\,\mathrm{km}^2$ (e.g. convection) and $500 \times 500\,\mathrm{km}^2$ (e.g. coastal convergence, pollution transport in the regional scale). Within METRAS the gas-phase and aerosol chemistry is simultaneously solved with the wind, temperature and humidity fields. Studies performed with METRAS focused on mesoscale phenomena, on pollution transport and the processes influencing deposition (Schlünzen, 1990; Wu and Schlünzen, 1992; Niemeier and Schlünzen, 1993; Schlünzen et al., 1997; von Salzen and Schlünzen, 1999; Sheng et al., 2000). The influence of various parameterisations on model results has been studied (Schlünzen and Pahl, 1992; Lüpkes and Schlünzen, 1996; von Salzen et al., 1996), and the dependence of model results on boundary values has been investigated (Lenz et al., 2000). Model results have been compared with measurements and analytic solutions (Schlünzen, 1997).

3.2.1. Equations and parameterisations of METRAS. METRAS is a non-hydrostatic, three-dimensional mesoscale-β model, based on the fully prognostic equations for wind, temperature and humidity, cloud- and rainwater as well as pollutant concentrations (Schlünzen, 1990; Schlünzen et al., 1996). Pressure is calculated from the (diagnostic) anelastic approximation. The exchange coefficients are calculated with a mixing length approach for stable stratification and with a countergradient scheme for unstable stratification (Lüpkes and Schlünzen, 1996). The dry deposition of pollutants is calculated from a resistance model and depends on pollution and land-use characteristics (Schlünzen and Pahl, 1992). Chemical transformations are included in different complexity in the model (Niemeier, 1997; von Salzen and Schlünzen, 1999).

The equations are solved on an Arakawa C-grid in a boundary following

$$\eta = z_t(z - z_s)/(z_t - z_s)$$

coordinate system. METRAS may be nested in results of a coarser resolution model (e.g. weather forecast or regional climate model; Lenz et al., 2000), but the present simulations were performed with open lateral model boundaries to be as independent as possible from results of other models. Thus, zero boundary normal gradients are used for all variables except the boundary normal wind components. These are calculated from the prognostic momentum equations, using for avection upstream conditions at the downstream and radiation conditions (Orlanski, 1976) at the upstream boundary (Lüpkes and Schlünzen, 1996). With the employed grid staggering and numerical schemes the selected boundary conditions result in variable fluxes at the lateral boundaries. At the model top a rigid lid is implemented using absorbing layers to avoid reflection of vertically propagating waves. For this purpose a linear diffusion term is employed in the uppermost five layers, with the diffusion coefficient increasing towards the model top. As a result of non-linear interaction the influence of the absorbing layers

Table 2. *Parameters albedo,* A*, thermal diffusivity,* κ*, thermal conductivity,* ν*, soil/vegetation water availability,* α*, saturation value for soil/vegetation water,* W*, and roughness length for momentum,* z_0*, in the soil/vegetation surface model of the METRAS model simulations*

Land-use type	A (%)	κ (10^{-6} m^2 s^{-1})	ν [J (K m)$^{-1}$]	α (start value) (%)	W (m)	z_0 (m)
Water	[a]	0.15	100	49	100	[b]
Sand	20	0.57	1.05	5	0.026	0.0012
Mixed	20	0.52	1.33	10	0.138	0.04
Meadows	20	0.52	1.33	20	0.015	0.02
Heath	15	0.24	0.30	5	0.423	0.05
Bushes	20	0.52	1.33	15	0.081	0.10
Mixed forest	20	0.80	2.16	15	0.121	1.00
Coniferous forest	10	0.80	2.16	15	0.161	1.20
Urban/suburban	15	2.30	4.60	2.5	0.968	0.70

[a]Dependent on zenith angle.
[b]Charnock (1995).

was found in the model results down to 10 layers below the model top.

The surface energy and the surface humidity budget are both solved by using the force-restore method of Deardorff (1978). Prognostic equations are used for both, surface temperature (Schlünzen, 1990) and soil water availability, thereby including the effect of vegetation and soil in one layer. The surface characteristics albedo, thermal diffusivity, thermal conductivity, soil/vegetation water availability, saturation value for soil/vegetation water and roughness length are considering the effect of both, the soil and the vegetation on surface temperature and humidity changes.

In each grid cell, up to ten different land-use types may be included. These are distinguished by their albedo, thermal diffusivity, thermal conductivity, soil/vegetation water availability, saturation value for soil/vegetation water, and roughness length z_0 for momentum (Table 2). The roughness length for water vapour and temperature is calculated from z_0 following Brutsaert (1975). Two alternative parameterisations are available to account for the sub-grid-scale land use: parameter averaging and flux aggregation. For the parameter averaging method, the characteristic parameters are averaged considering the fractional sub-grid-scale land use. The surface fluxes of heat and momentum are then calculated from the average parameters using surface-layer similarity theory. More elaborate is the flux aggregation method, where surface fluxes and the blending height are separately calculated for each sub-grid-scale land use following Claussen (1991). From these sub-grid-scale fluxes grid-averaged fluxes are derived by considering the fractional coverage. The grid-averaged fluxes based on parameter averaging and on flux aggregation can be quite different. In addition, the average heat flux might even be against the heat fluxes calculated from average temperature gradients (Schmidt's paradox; Lettau, 1979). With flux aggregation the fluxes are less resolution dependent if the turbulent fluxes in the convective planetary boundary layer are reasonably well simulated (von Salzen et al., 1996).

3.2.2. Description of the METRAS model simulations. Several model simulations were performed with METRAS to study the effect of sub-grid-scale land-use effects on the surface parameters (Table 1). The simulations were performed with a horizontal resolution of either 4 or 18 km. The vertical resolution is 20 m close to the surface, with the lowest model level in a height of 10 m above ground. The vertical grid size is increasing with height (increasing factor 1.175) up to a maximum vertical grid size of 1000 m. Nineteen grid levels are within the lowest 2000 m in a height of about 10, 30, 50, 80, 110, 140, 190, 240, 300, 360, 440, 540, 650, 780, 850, 1100, 1330, 1580 and 1900 m. With the model top at 10 km and the used vertical resolution the absorbing layers begin 5500 m above ground. They influence the model results by non-linear interaction down to about 4000 m.

The nine sub-grid-scale land-use types of the study area were considered in the METRAS simulations (Fig. 2a). Flux aggregation was applied in simulations M1, M2, M7 and M8 to calculate the influence of sub-grid-scale fluxes when multiple land-use types were present per grid cell. In contrast, the simulations M3 and M4 applied the parameter averaging method.

Simulations M5 and M6 only used the main land-use type per grid cell and neglected sub-grid-scale land-use effects (Fig. 2b for M5).

The METRAS simulations were completed without nesting, thus temporal and spatial changes in the large-scale situation are not covered in the simulations. The average large-scale situation was included in the simulations by using averaged rawinsonde data of Lindenberg station, taken at 1800 UTC, 21 July 1994, and 1800 UTC, 22 July 1994 (Fig. 4). For all simulations except M7 and M8 these profiles were input data to the one-dimensional (1-D) version of METRAS, which was integrated until stationarity. The balanced 1-D profiles were used as start values for the 3-D METRAS assuming horizontal homogeneity and using the diastrophism method (Pielke, 1984). This is a form of dynamic initialisation where the initially flat topography is increased during the initialisation phase to its final terrain height. During the initialisation all equations are solved on the boundary following grid, but the large-scale values are recalculated to ensure their horizontal homogeneity (Schlünzen et al., 1996). All simulations were started for 1800 UTC, 21 July 1994. For simulations M7 and M8 profiles were extracted for the Lindenberg site from ECMWF analysis (average values 1200 UTC 21 July 1994 and 0000 UTC 22 July 1994) and NCEP re-analysis (1800 UTC 21 July 1994; Fig. 4). The profiles were again used to initialise METRAS via the 1-D METRAS pre-processor.

The deep soil temperature has been prescribed as 14 °C for Potsdam station (52°23′N, 13°04′E), which is situated 41 m above sea level in the model. The value is corrected in the 3-D model for the local orography height, which can be either lower or higher than the Potsdam station, by assuming a dry adiabatic lapse rate. Water temperatures for all water surfaces in the model area were prescribed to 24 °C. The value was taken from the "Berliner Wetterkarte" (Freie Universität Berlin, 1994). The surface characteristics determined for north-west Europe are used in the simulations (Schlünzen et al., 1996) with the soil/vegetation water availability α reduced to the values in Table 2 to take into account the dry period of the simulated situation.

For comparing with routine surface measurements the METRAS model results were interpolated to the corresponding measurement site and height. In horizontal direction the values were interpolated from the four neighbouring model grid points by employing a bi-linear interpolation. The resulting 10 m wind values are directly taken for the evaluation. Temperature and humidity are needed at 2 m. These values are computed from the horizontally interpolated values at 10 m above ground and of each of the sub-grid-scale land uses, thereby considering the parameterisation applied. The computing did not solely employ the values of the actual land use of the measurement site. Pressure was recalculated to sea-level from the actual model grid point height using a dry adiabatic lapse rate.

4. Evaluation method

In order to evaluate the model simulations by comparing with the observed data, both the accuracy as well as how representative the measured data are has to be considered. While information on the accuracy is available, the representativeness is hardly known. Therefore, the values we use for evaluation represent a desired forecast accuracy A (Table 3). The values for A are taken from Cox et al. (1998; their Table 5).

Wind measurements at wind speeds below 1 m s^{-1} were neglected in the evaluation since the measurement uncertainty is too high. This was the case for 69 data points (wind speed zero or about 0.5 m s^{-1}). Analysis of the original data has shown that some unrealistic values were included in the data set that were outside the threshold values for wind direction and pressure given in Table 3. The rejected data (152 for wind direction, 13 for pressure) were not considered in the evaluation.

For comparing the performance of different model simulations, a hit rate H (in %) is calculated that considers the desired model accuracy A:

Table 3. *Accuracy,* A*, desired and accepted range of measurements*

Variable	Temperature (°C)	Dew point temperature (°C)	Wind speed (m s^{-1})	Wind direction	Pressure (hPa)
Accuracy A desired	±2	±2	±1	±30 °	±1.7
Threshold values: minimum to maximum	0 to 45	−10 to 45	1 to 8	0° to 360°, Wind^{-1} speed above 1 m s^{-1}	990 to 1100

$$H = \frac{100}{m} \times \sum_{i=1}^{m} n_i,$$

$$\text{with } n_i = \begin{cases} 1 & \text{for } |\text{ difference (measurement, model result)}| < A \\ 0 & \text{for } |\text{ difference (measurement, model result)}| \geq A \end{cases},$$

where m is the number of comparison data (381 data each for temperatures and dew point temperatures, 368 data for pressure, 312 data for wind speed, 229 data for wind direction). For each of the five variables, a single hit rate H is calculated ranging from 100% if all model results are within A of the observations to 0% if none are. A weighted hit rate H_w is calculated per model sensitivity study by weighting the single hit rates with the number of comparison data. Model results were evaluated for a 24-h period, starting from midnight on 22 July 1994.

The hit rate is a reliable overall measure for describing model performance. It is able to consider the measurement uncertainty, which is much more difficult to consider in the bias, the correlation coefficient or the root mean square error. While these assume Gaussian error distributions, the hit rate is distribution independent. However, the hit rate gives no insight into the error distribution of a simulation, but it is sufficient to decide on the overall model performance. In order to test the reliability of the single numbers for the hit rates, their sensitivity on the selected comparison data set has been tested by evaluating model results against reduced data sets (90% of the available observations). Six different test sets were compiled, with the neglected 10% of the data arbitrarily chosen. The resulting uncertainty of the hit rates is below 2% for all variables. Hence, hit rates differing within 2% are considered to be the same.

5. Model results

A summary of the validation using hit rates for all five variables and all simulations is shown in Table 4. In the discussion that follows, comparisons will be made of the hit rates between selected simulations that indicate certain sensitivities. In particular, the sensitivity to horizontal resolution (4 or 5 km versus 18 km), inclusion of sub-grid-scale land-use effects and initialisation are discussed. First, however, some general statements on the performance of the models are made.

Inspecting the hit rates for the various variables evaluated (temperature, T, dew point temperature, T_d, wind speed, *ff*, wind direction, *dd*, and mean sea-level pressure, MSLP) shows that MSLP was the best simulated, with hit rates near 100% for DARLAM and 95%

Table 4. *Hit rates (*H*) for the variables* T, T_d, ff, dd*, MSLP and average hit rate* H_w *for all sensitivity studies of DARLAM and METRAS*

Case	Characteristics (for details see Table 1)								
	a	b	c	T	T_d	*ff*	*dd*	MSLP	H_w
D1	18	E/E	inc	64	40	34	63	99	61
D2	18	E/E	N	48	14	28	59	100	50
D3	5	E/D1	inc	68	35	37	63	100	61
D4	18	N/N	inc	62	27	51	63	96	60
D5	18	N/N	N	56	6	41	64	99	52
M1	4	M	F	73	79	58	63	94	75
M2	18	M	F	75	79	56	64	95	75
M3	4	M	P	63	57	52	61	94	66
M4	18	M	P	37	29	51	60	96	54
M5	4	M	–	67	69	58	64	94	71
M6	18	M	–	67	57	55	63	95	68
M7	4	E	F	27	78	58	62	63	57
M8	4	N	F	29	48	54	43	70	49

[a]Resolution in km.
[b]Initialisation/boundary conditions (E, ECMWF; N, NCEP; M, measured profile).
[c]For D1–D5 soil moisture (inc, increased), for M1–M8 sub-grid-scale fluxes (F, flux aggregation; P, parameter averaging; –, not relevant).

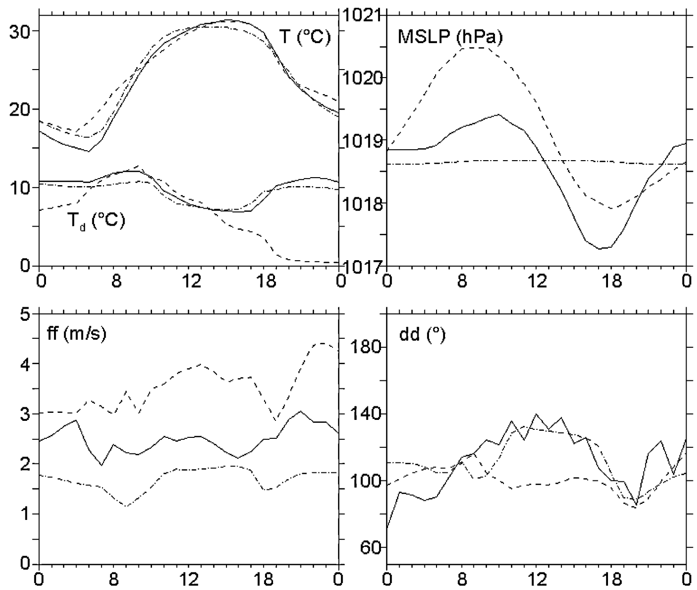

Fig. 5. Values of observed (solid line) and simulated (D1, dashed line; M1, dashed-dotted line) temperatures and dew point temperatures (top, left), mean sea-level pressure (top, right), wind speed (bottom, left) and wind direction (bottom, right) as average data from the 18 comparison sites.

for most of the METRAS simulations. Since DARLAM used the analysed data, which was created using the observations although modified by both the analysis model used and the multiple interpolations of the data to get them onto the model grid, it is not surprising that it captures the observed MSLP very well. The slightly lower values for the NCEP simulations were due to slightly higher pressure values in those analyses compared with the ECMWF and the observations. The METRAS model was initialised only with one value of surface pressure and not nested in larger-scale model results. Therefore METRAS could not capture the horizontal pressure gradient and the large-scale temporal change (Fig. 5). The fact that it does well indicates the pressure was quite uniform in the evaluation area, which was noted before and can be seen in Fig. 3.

The second-best variable simulated was wind direction, with hit rates on the order of 60%. With the fairly uniform easterly flow over the region (Fig. 3), this again could be expected. The fact that the hit rates are lower than for MSLP indicates that local influences are slightly more important for wind direction, primarily because the wind speed was quite low.

Temperature was also fairly well simulated, with an average hit rate of 57%. The better simulations have hit rates on the order of 75%. This is partly due to the fact that the temperature was strongly controlled by the solar heating during the daytime, which both models captured well (Fig. 5). In fact, most errors in the temperature were at night, where local configuration of orography and land use can cause significant differences in the development of the nocturnal boundary-layer and minimum temperatures.

Wind speed was the most difficult variable to simulate, with hit rates below 50% for DARLAM and slightly above 50% for METRAS. As with temperatures, the light wind conditions allow local, potentially unresolved, influences to be important. The simulated wind speeds are controlled by the local roughness length, which may not reflect the actual conditions at each site even when considering sub-grid-scale effects as in the METRAS simulations. However, the distribution of the differences has to be considered too. With a slightly enlarged accuracy A to about 1.5 m s^{-1} the hit rates increase considerably (METRAS, >70%; DARLAM, 50–70%). This increase seems plausible since a measuring reliability of 1 m s^{-1} is very high.

Although this study is not a model intercomparison, comments on the general performance of the two models give insight into model areas that need particular care. As noted above, in these simulations DARLAM used analyses as initial and boundary conditions while METRAS used a single profile, either an observed sounding or a sounding derived from the analyses. The general uniformity of the synoptic situation and lack of significant orography, clouds and rain allows both models to simulate the situation reasonably well. The main difference in validation between the models is in dew point temperature, with METRAS generally doing better. The dew point temperature is influenced by the boundary-layer moisture distribution, the soil moisture and land-use type. The differences in the validation between the models indicate that the complex interplay of the land-use type(s), soil moisture and temperature, both the initial specifications as well as their evolution in time, can lead to large differences in the dew point.

The model hit rates derived for DARLAM and METRAS compare well with hit rates based on the same criteria derived for other models and/or other case studies (Cox et al., 1998). For example, the average hit rates of four models is 35% for surface measurements in 12- to 36-h forecasts (Cox et al., 1998), with the wind speed showing the lowest hit rate (30%). The overall average of the single hit rates for the simulations D1–D5 and M1–M8 is 61% and for wind speed 49%.

5.1. Influence of horizontal resolution

The influence of horizontal resolution was investigated by comparing the model results for the higher-resolution simulations (4 km for METRAS and 5 km for DARLAM) with the corresponding lower resolution simulation (18 km). For DARLAM, the increase in horizontal resolution has no significant impact on wind and MSLP (cases D1 and D3), slightly increases the hit rate for temperature, but slightly decreases the hit rate for the dew point temperature. This suggests that a more accurate depiction of the surface characterisation at higher resolution leads to better simulation of some variables. The positive effect on the temperature was primarily the result of the better prediction of the nocturnal temperatures with higher resolution. All the DARLAM simulations tended to have decreases in dew point at night (Fig. 5), which were not observed. Evidently, the scheme used in these simulations created too much dew.

For METRAS, the simulations with the flux aggregation approach show little change with resolution (M1 and M2), all changes are below the 2% uncertainty of the hit rate. These results indicate that METRAS with sub-grid-scale land use and the blending height concept simulates the observed data equally well at both 4 and 18 km. The changes are still small, if only the main land-use type is considered (M5 and M6). However, when applying the parameter averaging to describe the sub-grid-scale land-use effects (M3 and M4), the performance of the model improves considerably when the resolution increases. The average hit rate of 54% for the 18-km simulation (M4) increases to 66% for the 4-km simulation (M3). The improvement results mainly from the improved forecast of the temperatures and dew point temperatures.

5.2. Influence of sub-grid-scale land-use effects

The impact of resolution discussed in the last section has shown an improvement for METRAS employing parameter averaging and slight changes with increased horizontal resolution for both models when they had only one land-use type per grid cell. No impact appeared for METRAS with aggregated sub-grid-scale fluxes. This suggests that the inclusion of the sub-grid-scale effects can ameliorate the degrading effects of decreased resolution. In this section results of METRAS simulations with various sub-grid-scale parameterisations included are discussed. The results include the previously discussed simulations that had sub-grid-scale effects and flux aggregation (M1 and M2), to sub-grid-scale land use but with parameter averaging (M3 and M4), and finally to no sub-grid-scale effects by allowing only one land-use per grid cell (M5 and M6) as in DARLAM. These results are evaluated at both the 4- and 18-km resolutions.

The 4-km METRAS simulation M3, which included the sub-grid-scale land use (Fig. 2a) but used parameter averaging, shows a decrease in hit rate compared with the simulation with the flux aggregation (M1). The wind field and MSLP show little change, but the temperatures and dew point temperatures show significant decreases in accuracy. Evidently, there is a greater impact of local land use on the surface fluxes of heat and moisture than on momentum. This results from the fact that surface drag is controlled by the surface roughness to a large degree, which does not depend on sub-grid-scale land use as strongly as the heat and moisture fluxes. While averaging of the surface roughness does not significantly impact the wind simulation, the averaging of surface parameters before computing surface fluxes of heat and moisture does not give results that are consistent with the aggregation of the surface fluxes using the correct parameters for each sub-grid-scale land use. In fact, these results indicate that averaging of parameters leads to less accurate surface fluxes when compared with the average fluxes from the various sub-grid-scale land-use areas.

These results can also be compared with the simulation using only the main land-use type for each grid cell (M5; Fig. 2b). In this simulation, no sub-grid-scale land-use effects are accounted for; each grid cell is assumed to have only one land-use type, like the DARLAM simulations. The results for these simulations show improvements compared to the parameter averaging simulation (M3) for all variables, apart from MSLP, which shows no change. However, comparing the one land-use type (M5) with the sub-grid-scale land use with flux aggregation (M1) shows that the one land-use simulation is worse for temperatures and dew point temperatures. This again confirms the importance of including the sub-grid-scale fluxes of heat and moisture properly. The wind fields are again very similar, indicating the lack of influence of sub-grid-scale effects on momentum. These results confirm the inappropriateness of parameter averaging for the computation of surface heat and moisture fluxes and the positive impact on temperature and moisture by including sub-grid-scale effects properly.

The degrading of the results when using parameter averaging is even more dramatic at the 18-km horizontal resolution simulation (M2 and M4). All parameters show a decrease in accuracy at this resolution when one goes from the flux aggregation to the parameter averaging. The strongest impact is again on temperatures and dew point temperatures. Only MSLP shows little change.

Comparing the results at 4- and 18-km horizontal resolutions clearly indicates that as the horizontal resolution decreases, the proper inclusion of sub-grid-scale effects becomes more important, at least for temperature and moisture. These results also suggest that the parameter averaging technique becomes less appropriate the larger the averaging area, and the greater the sub-grid-scale heterogeneity. In other words, the inclusion of sub-grid-scale heterogeneity by flux aggregation is less important at 4 km than at 18 km, but still has a positive impact.

5.3. Influence of initialisation on model results

Since all the simulations completed were for at most 36 h, the issue of the impact of initial conditions becomes relevant in discussing the results. To address these concerns, several additional simulations were completed in order to partly investigate the impact of the initial conditions on the results. Since the main emphasis of this study was on the impact of sub-grid-scale land-use effects, this discussion will only indicate the relative importance of the initial conditions compared with the impact of sub-grid-scale effects, not a thorough evaluation of the impact of initial conditions.

Two features of the initial conditions were investigated in the DARLAM simulations: the analysis used to initialise the model (either ECMWF standard analysis or NCEP re-analysis) and the initial soil moisture. The impact of the initial analysis used shows differing results depending upon the variable evaluated. In general, the ECMWF simulation (D1) was slightly better than the corresponding NCEP simulation (D4), except for wind speed. The most positive influence of using the ECMWF analyses was in the dew point temperature and to a lesser degree temperature. The wind speed in the simulation using ECMWF analyses was generally stronger, and less accurate, than the simulation using NCEP, partly because the pressure gradient was stronger. The surface roughness was identical in both simulations and so was not a factor.

Uncertainty in the initial soil moisture was also investigated. Although the NCEP re-analysis provided soil moisture, this field is not observed and very dependent upon the surface scheme and input specification of vegetation and soil type used in the re-analysis and on the accuracy of the rainfall data over the previous few days. The initial simulations (D2 and D5) were completed using the NCEP soil moisture, but it was found that the diurnal air temperature signal was too large and dew point temperatures were too low. Since it is well known that the impact of soil moisture on atmospheric parameters can be considerably (Zhang and Anthes, 1982; Klink and Willmott, 1994), its impact on the DARLAM simulation results was tested by setting the initial minimum soil moisture to 90% of the field capacity for each soil type specified in DARLAM, corresponding to 0.28 m^3 m^{-3}. This effectively increased the soil moisture in northern Germany and throughout the evaluation area by about 10% above that in the NCEP re-analyses. The positive impact of using this ‘corrected’ soil moisture can be seen in both temperatures. The impact on the temperature is an indirect effect, since the amount of soil moisture will influence the partitioning of the surface energy fluxes between latent (which effects dew point temperature) and sensible (which effects temperature). Given that the amount of incoming energy (downward longwave and shortwave radiation) was basically the same, the simulation with larger soil moisture will cause increases in latent heat fluxes and higher dew points and corresponding decreases in sensible heat fluxes and lower daytime temperatures. These changes make the simulation with larger soil moistures more accurate. There was also a positive impact on the wind fields. This was caused by changes in the development of the boundary-layer depth which resulted from the temperature changes noted above. Note that the impact of changes in soil moisture (D1 and D2) was larger than of the change in resolution (D1 and D3), while the influence of the initial conditions (D1 and D4) was only slightly greater than the influence of resolution.

In order to show the impact of initial conditions on the METRAS simulation results, the model was initialised using an equivalent sounding extracted from the analyses for a point nearest Lindenberg radiosonde site. There was a marked negative impact on the temperatures using these soundings; they were the least accurate of all completed (M7 and M8). This is partly a result of differences in the initial boundary-layer temperatures, both of which were lower than when using the observed sounding (Fig. 4). The impact on the dew point was very small for the simulation using ECMWF data (M7), but again much worse when using the NCEP sounding (M8). This is consistent with the sensitivity in the DARLAM simulations to initial analysis. The impact on the winds was small, while there was a negative impact on the MSLP. Both analyses had MSLPs 1 hPa, larger than the rawinsonde profile used in the other METRAS simulations. This resulted in an average overestimation of the surface pressure by 1 hPa which again resulted in a degrading of the model hit rate (accepted accuracy 1.7 hPa).

For the METRAS simulations, the impact of the assumed initial profile was generally larger than for the various sub-grid-scale sensitivity simulations as long as parameter averaging was avoided. The METRAS simulation M8 initialised using the NCEP sounding was worse than all other simulations. The simulation M7 initialised with the ECMWF sounding was worse for temperature, but the other variables were comparable to the observed sounding simulations.

The conclusion from these simple sensitivity simulations indicates that for these short-term forecasts, the initial conditions can have a significant impact on the resulting simulation results. The conclusions on the influence of sub-grid-scale land-use have therefore to be based on model simulations using the same initialisation.

6. Conclusions

This paper investigates the impact of various sub-grid-scale land-use parameterisations for simulations with different horizontal resolution. Two models were evaluated for the same situation: DARLAM, a regional model designed primarily for climate studies, and METRAS, a high-resolution, non-hydrostatic model designed primarily for pollution studies. DARLAM does not have a sub-grid-scale surface scheme, and therefore allows only one main land use and bare ground per grid cell. METRAS has alternative schemes to account for sub-grid-scale land-use effects (parameter averaging or flux aggregation with blending height concept). The use of these two models allowed the comparison of various strategies and model formulations and their impact on the simulation of temperatures and dew point temperatures, wind and mean sea-level pressure.

The models were compared with station observations in the area around Berlin, Germany, for a 24-h period on 22 July 1994. Around this time, there was nearly steady, weak easterly flow with relatively dry air and few clouds over the region, so local land-use effects would dominate large-scale advection. The models were evaluated by comparing the surface station observations to the corresponding model result data (interpolated 2- or 10-m values). The observations were first evaluated to eliminate unrealistic values. An acceptable accuracy was then established for temperatures and dew point temperatures, wind and mean sea-level pressure in order to establish the 'hit rate' of the models. This describes the percentage of model results which were within the acceptable range of the observations.

Both models generally show little changes with increasing resolution (18 to 4 or 5 km), if only one main vegetation type is considered. If sub-grid-scale land characteristics are included, the type of inclusion is significant: the METRAS simulations which used parameter averaging as a means to account for sub-grid-scale effects show a positive impact of increasing resolution, but the results were in fact worse than the simulations where only the main land use was assigned to each grid cell. When including sub-grid-scale land use and using the flux aggregation, the METRAS model also had no significant change in model performance with resolution, but shows the highest hit rates and thus the best results. This indicates that including sub-grid-scale land-use effects in models can produce a more accurate simulation of especially temperatures and dew point temperatures.

The impact of the initial state was also briefly investigated and did show significant impact for both models. For DARLAM, the more significant impact was related to the soil moisture. For METRAS, using open lateral boundaries, the impact of the initial atmospheric profile was very large. The conclusions drawn on resolution and sub-grid-scale land-use effect parameterisations are therefore based on simulations of same initial data.

The comparisons of the results with measurements have shown that initial soil moisture and treatment of sub-grid-scale land-use characteristics are both important for temperatures and dew point temperatures, and less so for winds and mean sea-level pressure. In summary, the following are the main conclusions of this study: (1) Increasing resolution does not necessarily improve model performance but might help, if insufficient parameterisations (here: parameter averaging) are applied. (2) Sub-grid-scale parameterisation with flux aggregation and blending heights increases model performance and helps for scale-independence of model results. (3) Initialisation is important for these short-term simulations.

While the performance of the two models changes consistently for initial data, the reaction on increasing resolution depends on the parameterisation applied for sub-grid-scale land-use effects. METRAS seems to perform well for the resolutions tested, and is resolution independent with the flux aggregation scheme. The differences in model performance will probably decrease for more large-scale driven meteorological situations (e.g. stronger winds), when local, sub-grid-scale vertical transport might be less intense than the horizontal advective transport.

The results suggest that a more complex calculation of the surface fluxes might also improve the DARLAM results for the resolutions used. Future work will thus investigate the resolution dependence of sub-grid-scale fluxes and the impact of the sub-grid-scale flux aggregation on the DARLAM simulations. Eventually, the impact of the sub-grid-scale land-use effects on the development of the boundary layer will be studied. In addition, other cases will be investigated in order to verify the generality of these results.

7. Acknowledgements

The measurements were kindly provided by the "Deutscher Wetterdienst." Assistance of the Australian–German collaboration agreement to help facilitate the interaction of the scientists is greatly appreciated (BMBF project AUS-022). Thanks go to the reviewers for their comments and suggestions.

REFERENCES

Arakawa, A. 1972. Design of the UCLA general circulation model. Numerical simulation of weather and climate. *Tech. Report No. 7*, Department of Meteorology, University of California Los Angeles, USA.

Arola, A. 1999. Parametrisaton of turbulent and mesoscale fluxes for heterogeneous surfaces. *J. Atmos. Sci*. **56**, 584–598.

Bélair, S., Lacarrére P., Noilhan J., Masson V. and Stein J. 1998. High resolution simulation of surface turbulent fluxes during HAPEX-MOBILHY. *Mon. Wea. Rev*. **126**, 2234–2253.

Brutsaert, W. 1975. The roughness length for water vapor, sensible heat and other scalars. *J. Atmos. Sci*. **32**, 2028–2031.

Charnock, H. 1955. Wind stress on a water surface. *Q. J. R. Meteorol. Soc*. **81**, 639–640.

Claussen, M. 1991. Estimation of areally-averaged surface fluxes. *Boundary-Layer Meteorol*. **54**, 387–410.

Cox, R., Bauer, B. L. and Smith, T. 1998. Mesoscale model intercomparison. *Bull. Am. Meteorol. Soc*. **79**, 265–283.

Davies, H. C. 1976. A lateral boundary formulation for multi-level prediction models. *Q. J. R. Meteorol. Soc*. **102**, 405–418.

Deardorff, J. W. 1978. Efficient prediction of ground surface temperature and moisture, with inclusion of a layer of vegetation. *J. Geophys. Res.* **83**, 1889–1903.

Freie Universität Berlin Institut für Meteorologie 1994. Berliner Wetterkarte im Jahre 1994. *Meterologische Abhandlungen, Neue Folge, Serie B, Grundlagenmaterial*; **71–7**, Verlag Dietrich Reimer, Berlin.

Katzfey, J. J. 1995. Simulation of extreme New Zealand precipitation events. Part 1: Sensitivity to orography and resolution. *Mon. Wea. Rev*. **123**, 737–754.

Katzfey, J. J. and Ryan, B. F. 1996. Modification of the thermodynamic structure of the lower troposphere by the evaporation of precipitation: A GEWEX cloud system study. *Mon. Wea. Rev*. **125**, 1431–1466.

Katzfey, J. J. and Ryan, B. F. 2000. Midlatitude frontal clouds: GCM-Scale Modeling Implications. *J. Climate* **13**, 2729–2745.

Klink, K. 1995. Surface aggregation and subgrid-scale climate. *Int. J. Climatol*. **15**, 1219–1240.

Klink, K. and Willmott, C. J. 1994. Influence of soil moisture and surface roughness heterogeneity on modeled climate. *Climate Res*. **4**, 105–113.

Kowalczyk, E. A., Garratt, J. R. and Krummel, P. B. 1991. A soil-canopy scheme for use in a numerical model of the atmosphere-1D stand-alone model. *Tech. Paper*. **23**, CSIRO Div. Atmos. Res., PMB1, Aspendale, Vic. 3195, Australia.

Lacis, A. A. and Hansen, J. E. 1974. A parameterization for the absorption of the solar radiation in the Earth's atmosphere. *J. Atmos. Sci*. **31**, 118–133.

Lenz, C.-J., Müller, F. and Schlünzen, K. H. 2000. The sensitivity of mesoscale chemistry transport model results to boundary values. *Environ Monitoring and Assessment* **65**, 287–295.

Lettau, H. H. 1979. Wind and temperature profile prediction for diabatic surface layers including strong inversion cases. *Boundary-Layer Meteorol*. **17**, 443–464.

Louis, J-F. 1979. A parametric model of vertical eddy fluxes in the atmosphere. *Boundary-Layer Meteorol*. **17**, 187–202.

Lynn, B. H., Rind, D. and Avissar, R. 1995. The importance of mesoscale circulations generated by subgrid-scale landscape heterogeneities in general circulation models. *J. Climate* **8**, 191–205.

Lüpkes, C. and Schlünzen, K. H. 1996. Modelling the Arctic convective boundary-layer with different turbulence parameterizations. *Boundary-Layer Meteorol*. **79**, 107–130.

McGregor, J. L. 1987. Accuracy and initialization of a two-time-level split semi-Lagrangian model. In: *Short- and medium-range numerical weather prediction* (ed. T. Matsuno), *J. Meteorol. Soc. Jpn. Special Volume*, 233–246.

McGregor, J. L. 1993. Economical determination of departure points for semi-Lagrangian models. *Mon. Wea. Rev*. **121**, 221–246.

McGregor, J. L., Walsh, K. J. and Katzfey, J. J. 1993.Nested modelling for regional climate studies. In: *Modelling change in environmental systems* (eds. A. J. Jakeman, M. B. Beck and M. J. McAleer) Wiley, New York, 367–386.

Mölders, N., Raabe, A. and Tetzlaff, G. 1996. A comparison of two strategies on land surface heterogeneity used in a mesoscale beta meteorological model. *Tellus* **48A**, 733–749.

Müller, F., Schlünzen, K. H. and Schatzmann, M. 2000. Test of numerical solvers for chemical reaction mechanisms in 3D air quality models. *Environmental Modelling Software* **15**, 639–646.

Niemeier, U. 1997. Chemische Umsetzungen in einem hochauflösenden mesoskaligen Modell–Bestimmung geeigneter Randwerte und Modellanwendungen -. *Dissertation, Fachbereich Geowissenschaften, Universität Hamburg* **A28**, 161 pp.

Niemeier, U. and Schlünzen, K. H. 1993. Modelling steep terrain influences on flow patters at the Isle of Helgoland. *Beitr. Phys. Atmosph*. **66**, 45–62.

Orlanski, I. 1976. A simple boundary condition for unbounded hyperbolic flows. *J. Comput. Phys*. **21**, 251–269.

Pielke, R. A. 1984. *Mesoscale meteorological modeling*. Academic Press, London, 612 pp.

Schlünzen, K. H. 1990. Numerical studies on the inland penetration of sea breeze fronts at a coastline with tidally flooded mudflats. *Beitr. Phys. Atmosph*. **63**, 243–256.

Schlünzen, K. H. 1997. On the validation of high-resolution atmospheric mesoscale models. *J. Wind Eng. Ind. Aerodynam*. **67&68**, 479–492.

Schlünzen, K. H. and Pahl, S. 1992. Modification of dry deposition in a developing sea-breeze circulation–a numerical case study. *Atmos. Environ*. **26A**, 51–61.

Schlünzen, K. H., Bigalke, K., Lüpkes, C., Niemeier, U. and Salzen, K. 1996. Concept and realization of the mesoscale transport- and fluid-model 'METRAS'. *METRAS Techn. Rep., Meteorologisches Institut, ZMK, Universität Hamburg* **5**, 156 pp.

Schlünzen, K. H., Stahlschmidt, T., Rebers, A., Niemeier, U., Kriews, M. and Dannecker, W. 1997. Atmospheric input of lead into the German Bight–A high resolution measurement and model case study for April 23rd to 30th, 1991. *Mar. Ecol. Prog. Ser*. **156**, 299–309.

Schwarzkopf, M. D., and Fels, S. B. 1991. The simplified exchange method revisited: An accurate, rapid method for computation of infrared cooling rates and fluxes. *J. Geophys. Res.* **96**, 9075–9096.

Sheng, L., Schlünzen, K. H. and Wu, Z. 2000. Three-dimensional numerical simulation of the mesoscale wind structure over Shandong peninsula. *Acta Meteorol. Sinica* **1**, 97–107.

Smiatek, G. 1998. Mapping land-use for modelling biogenic and anthropogenic emissions. Proceedings of the EUROTRAC2 Symposium, Garmisch-Partenkirchen.

USGS, 1996. Global digital elevation model GTOPO30. U.S. Geological Survey, EROS Data Center in Sioux Falls, South Dakota.

Salzen, K. and Schlünzen, K. H. 1999. Simulation of the dynamics and composition of secondary and marine inorganic aerosols in the coastal atmosphere. *J. Geophys. Res.* **D23**, 30 201–30 217.

Salzen, K., Claussen, M. and Schlünzen, K. H. 1996. Application of the concept of blending height to the calculation of surface fluxes in a mesoscale model. *Meteorol. Z*. **NF5**, 60–66.

Wu, Z. and Schlünzen, K. H. 1992. Numerical study on the local wind structures forced by the complex terrain of Qingdao area. *Acta Meteorol. Sinica* **6**, 355–366.

Zeng, X. and Pielke, R. 1995. Landscape-induced atmospheric flow and its parameterization in large-scale numerical models. *J. Climate* **8**, 1156–1177.

Zhang, D. and Anthes, R. 1982. A high-resolution model of the planetary boundary layer: sensitivity tests and comparisons with SESAME-79 data. *J. Appl. Meteorol*. **21**, 1594–1609.